

Electrical properties for poly-Ge films fabricated by pulsed laser annealing

Hajime Watakabe^{a,*}, Toshiyuki Sameshima^a, Hiroshi Kanno^b, Masanobu Miyao^b

^a Tokyo University of Agriculture and Technology, 2-24-16 Nakacho, Koganei, Tokyo 184-8588, Japan

^b Dept. of Electronics, Kyushu University, 6-10-1 Hakozaki, Fukuoka 812-8581, Japan

Available online 16 November 2005

Abstract

Electrical properties of 50-nm-thick polycrystalline germanium (poly-Ge) films fabricated by pulsed laser annealing were investigated. Analysis of the electrical conductivity using a numerical calculation program revealed that the density of defect states at grain boundaries in the poly-Ge films was a low of $1.1 \times 10^{12} \text{ cm}^{-2}$ in contrast to a high density of $2.6 \times 10^{13} \text{ cm}^{-2}$ in the case of laser crystallized poly-Si films. Transient photoconductivity measurements using pulsed laser irradiation revealed that 50-nm-thick poly-Ge films had a long carrier lifetime of 3.0 μs .

© 2005 Elsevier B.V. All rights reserved.

Keywords: Laser irradiation; Germanium; Grain boundary; Photoconductivity

1. Introduction

Formation of polycrystalline germanium (poly-Ge) films by pulsed laser irradiation is attractive for its application to thin film transistors (TFTs) because crystalline germanium have high electron and hole mobilities than those of crystalline silicon. Poly-Ge TFTs with high carrier mobility have a possibility to realize high speed electrical circuits on glass substrate [1,2]. However, electrical and structural properties of laser crystallized poly-Ge films have not been investigated enough. In this paper, we discuss electrical properties of poly-Ge films fabricated by pulsed laser annealing. Analysis of the density of electrically active defect states at grain boundaries is discussed. Transient photoconductivity measurements are also reported.

2. Experimental

Amorphous germanium (a-Ge) films with a thickness of 50 nm were formed on quartz substrate by the method of plasma sputtering. Amorphous silicon (a-Si) films were also formed by the low pressure chemical vapor deposition (LPCVD) method for the reference. Boron atoms were implanted with concentrations of 5.0×10^{17} and $1.0 \times 10^{18} \text{ cm}^{-3}$ by the ion doping method at an acceleration energy of 10 keV. The films were

crystallized by 30-ns-pulsed XeCl excimer laser irradiation at room temperature in vacuum. 5-shots multiple step laser irradiations were carried out. The laser energy density was increased stepwise from 90 to 180 mJ/cm^2 with a 10 mJ/cm^2 steps for a-Ge films and from 150 to 425 mJ/cm^2 with a 25 mJ/cm^2 steps for a-Si films. After laser irradiation, the crystalline volume fraction was estimated by the analysis of optical reflectivity spectra in ultraviolet region [3]. Crystalline silicon and germanium have a broad optical peak at around 276 nm, which is caused by the large transition rate at the X point in the band structure. The crystalline volume fraction, C , was defined by the following equation,

$$n_p = (1 - C)n_a + Cn_c \quad (1)$$

where n_p , n_a and n_c are the complex refractive index for polycrystalline, amorphous and single crystalline germanium or silicon, respectively. The crystalline volume fraction was obtained by the fitting of calculated reflectivity spectra to experimental reflectivity spectra. The crystalline volume fraction, C , was estimated to be 0.90 for poly-Ge films crystallized at 180 mJ/cm^2 and 0.84 for poly-Si films crystallized at 425 mJ/cm^2 . Al gap electrodes were formed by vacuum evaporation with a width of 0.10 cm and a length of 0.18 cm. In order to reduce electrically active defect states in the polycrystalline films, 13.56 MHz hydrogen plasma treatment was carried out at 30 W, 130 Pa, 250 °C and for 30 s [4–6]. Numerical calculation program was developed

* Corresponding author. Tel.: +81 42 388 7436; fax: +81 42 388 7436.

E-mail address: watakabe@cc.tuat.ac.jp (H. Watakabe).

using the finite element method with statistical thermodynamical conditions to estimate defect states at grain boundaries in the poly-Ge and poly-Si films [7–9]. The defect states were localized at grain boundaries, which distributed uniformly in the bandgap. The crystalline grain size was assumed as 126 nm for poly-Ge films and 50 nm for poly-Si films on the base of our previous investigation [10,11]. Analysis of experimental conductivity with different temperatures by the numerical calculation program gave the density of defect states in the bandgap.

3. Results and discussion

Fig. 1 shows electrical conductivity as a reciprocal function of absolute temperature for poly-Ge films (a) and poly-Si films (b) with boron-doping concentrations of 0 (non-doped), 5.0×10^{17} and $1.0 \times 10^{18} \text{ cm}^{-3}$. Fig. 1b also shows electrical conductivity for $1.0 \times 10^{18} \text{ cm}^{-3}$ doped poly-Si film after hydrogen plasma treatment. High electrical conductivities were observed in the every doping concentration as shown in Fig. 1a. The electrical conductivity reduced from 3.5 to 0.84 S/cm as the doping concentration increased from 0 to $5.0 \times 10^{17} \text{ cm}^{-3}$ at room temperature. On the other hand, it increased to 13.6 S/cm as doping concentration increased to

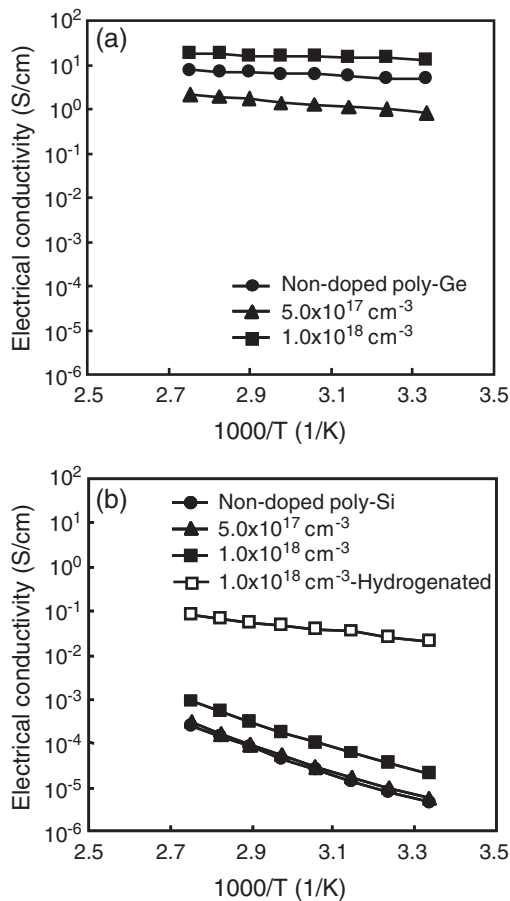


Fig. 1. Electrical conductivity as a reciprocal function of absolute temperature for poly-Ge films (a) and poly-Si films (b) with boron-doping concentration of 0 (non-doped), 5.0×10^{17} and $1.0 \times 10^{18} \text{ cm}^{-3}$.

Table 1

Densities of defect states at grain boundaries, potential barrier height, effective hole density to the lateral direction and effective hole mobility obtained by the numerical analysis

	Poly-Ge as-crystallized	Poly-Si as-crystallized	Poly-Si hydrogenated
Density of defect states (cm^{-2})	1.1×10^{12}	2.6×10^{13}	4.1×10^{12}
Potential barrier height (eV)	0.039	0.38	0.15
Effective hole density (cm^{-2})	1.4×10^{12}	1.2×10^7	1.3×10^{11}
Effective hole mobility ($\text{cm}^2/\text{V s}$)	295	59	77

$1.0 \times 10^{18} \text{ cm}^{-3}$. These results show that poly-Ge films were sensitive to boron doping. Decrease of the electrical conductivity by $5.0 \times 10^{17} \text{ cm}^{-3}$ -boron doping suggests that Ge films were initially doped with uncontrolled donor species. Analysis of electrical conductivities using the numerical calculation program revealed that the donor density was $4.3 \times 10^{17} \text{ cm}^{-3}$. Poly-Ge film doped with $5.0 \times 10^{17} \text{ cm}^{-3}$ boron atoms is therefore near intrinsic states. No significant change in the electrical conductivity was observed by hydrogen plasma treatment for non-doped and every doping case. On the other hand, the electrical conductivity was a very low of $4.6 \times 10^{-6} \text{ S/cm}$ for the non-doped poly-Si film at room temperature. The electrical conductivity was slightly increased to $2.0 \times 10^{-5} \text{ S/cm}$ as doping concentration increased to $1.0 \times 10^{18} \text{ cm}^{-3}$. Hydrogen plasma treatment markedly increased the electrical conductivity to 0.019 S/cm. Moreover, the slope of the electrical conductivity with temperature decreased. These results indicate that the hydrogen plasma treatment reduced activation energy with reduction of electrically active defect states at grain boundaries.

Table 1 shows the densities of defect states at grain boundaries, potential barrier height, effective hole density to the lateral direction and effective hole mobility obtained by the analysis of electrical conductivity using the numerical calculation program for as-crystallized poly-Ge films, as-crystallized poly-Si films and hydrogenated poly-Si films doped with $1.0 \times 10^{18} \text{ cm}^{-3}$. The density of defect states at grain boundaries was estimated to be $1.1 \times 10^{12} \text{ cm}^{-2}$ for as-crystallized poly-Ge films. The low defect density resulted in a low potential barrier height, 0.039 eV and a high effective hole density, $1.4 \times 10^{12} \text{ cm}^{-2}$. Moreover, the effective carrier mobility was as high as 295 $\text{cm}^2/\text{V s}$. On the other hand, the defect density at grain boundary was estimated to be $2.6 \times 10^{13} \text{ cm}^{-2}$ for as-crystallized poly-Si films. This high density of defect states resulted in a high potential barrier height, 0.38 eV and a low effective hole density, $1.2 \times 10^7 \text{ cm}^{-2}$. Hydrogen plasma treatment effectively reduced the defect density to $4.1 \times 10^{12} \text{ cm}^{-2}$. The effective carrier mobility was 77 $\text{cm}^2/\text{V s}$. From these results, the density of defect states at grain boundary in the poly-Ge films is lower than that of hydrogenated poly-Si films. Moreover, the effective hole mobility was also high probably because crystalline germanium have four times higher hole mobility than that of silicon

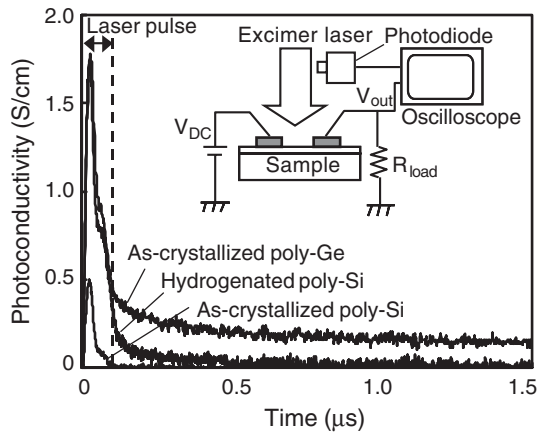


Fig. 2. Changes in the photoconductivity for as-crystallized poly-Ge films, as-crystallized poly-Si films and hydrogenated poly-Si films with a boron-doping concentration of $1.0 \times 10^{18} \text{ cm}^{-3}$. The laser energy density for generation of photo carrier was 1.2 mJ/cm^2 . The inset shows the electrical circuit for the measurement of transient photoconductivity.

[12]. In order to analyze photo-induced carrier responses, transient photoconductivity induced by pulsed laser irradiation was measured. Fig. 2 shows changes in the photoconductivity for as-crystallized poly-Ge, as-crystallized poly-Si film and hydrogenated poly-Si film doped with $1.0 \times 10^{18} \text{ cm}^{-3}$. The electrical conductivity before laser irradiation was subtracted in every case. The photoconductivity was measured using simple electrical circuit as shown in an inset. DC voltage was applied to the samples. The transient photocurrent was measured as a voltage at the load resistance connected between sample and ground using a 1 GHz high-speed digital oscilloscope. Photo carriers were generated by pulsed XeCl excimer laser irradiation with laser energy density of 1.2 mJ/cm^2 , which was much smaller than threshold laser energy density for crystallization of a-Ge and a-Si [13]. Change in the laser power intensity was also monitored using photodiode. The laser pulse was initiated at 0 s and finished at about 100 ns. The photoconductivities rapidly increased in a coincidence with the initiation of the laser irradiation for all samples as shown in Fig. 2. The peak conductivity for poly-Ge film was 1.70 S/cm . After the peak conductivity, it decreased immediately. However, the photoconductivity was still observed after termination of laser pulse. This result indicates that photo carriers have a long carrier lifetime because of low recombination ratio associated with a low defect density at grain boundaries as well as the sample surface. On the other hand, as-crystallized poly-Si films have a low peak conductivity at 0.48 S/cm . The photoconductivity was not observed within the instrumental resolution after termination of laser pulse. Photo carriers have a very low carrier lifetime because of high recombination ratio associated with a high defect density. Hydrogen plasma treatment markedly increased the peak conductivity to 1.68 S/cm . The photoconductivity was observed after termination of laser pulse. Hydrogen plasma treatment reduced defect states at grain boundary and increased the carrier lifetime. For estimating of the photo carrier lifetime, the photoconductivity after termination of laser pulse was analyzed. If the photo

carrier reduction rate is proportional to the density of recombination sites, N_t , and photoconductivity as,

$$\frac{d\sigma_p}{dt} = -AN_t\sigma_p \quad (2)$$

where A is a constant. The photoconductivity, σ_p , is described as,

$$\sigma_p = B \exp(-AN_t t) = B \exp\left(-\frac{t}{\tau}\right) \quad (3)$$

where B is the constant, τ , is the carrier lifetime. The lifetime was estimated by the fitting of calculated photoconductivity obtained by the Eq. (3) to the experimental photoconductivity decay after termination of laser pulse. The lifetimes were estimated to be $3.0 \mu\text{s}$ and $0.45 \mu\text{s}$ for poly-Ge film and hydrogenated poly-Si film, respectively. From Eqs. (2) and (3), the lifetime will be a reciprocal function of density of recombination sites. Therefore, the lifetime of poly-Ge films was 6.7 times ($=3.0 \mu\text{s}/0.45 \mu\text{s}$) of that of hydrogenated poly-Si films. Table 1 gave the ratio of the density of defect states of N_t (hydrogenated poly-Si)/ N_t (poly-Ge). It was about 4. These estimations suggest that the low density of recombination sites resulted in long carrier lifetime in poly-Ge films associated with the low density of defect states at grain boundaries.

4. Summary

We investigated the electrical properties of 50-nm-thick poly-Ge films fabricated by the pulsed laser annealing. Analysis of electrical conductivity using the numerical calculation program revealed that the density of defect states at grain boundary in as-crystallized poly-Ge films was a low of $1.1 \times 10^{12} \text{ cm}^{-2}$. The effective carrier mobility was also high at $295 \text{ cm}^2/\text{V s}$. On the other hand, the density of defect states in the poly-Si films was $2.6 \times 10^{13} \text{ cm}^{-2}$. Transient photoconductivity measurement revealed that the carrier lifetime of poly-Ge films was 6.7 times that of hydrogenated poly-Si films. These results show a possibility to fabricate poly-Ge TFTs with high mobility.

References

- [1] S. Uchikoga, N. Ibaraki, Thin Solid Films 383 (2001) 19.
- [2] K. Kanzaki, AM-LCD'01, 2001, p. 71.
- [3] T. Sameshima, K. Saitoh, N. Aoyama, S. Higashi, M. Kondo, A. Matsuda, Jpn. J. Appl. Phys. 38 (1999) 1892.
- [4] T. Sameshima, M. Sekiya, M. Hara, N. Sano, J. Appl. Phys. 76 (1994) 7377.
- [5] K. Kitahara, K. Nakajima, A. Moritani, Jpn. J. Appl. Phys. 40 (2001) 1209.
- [6] Y.S. Kim, K.Y. Choi, M.K. Han, J. Appl. Phys. 34 (1995) 719.
- [7] P.V. Evans, S.F. Nelson, J. Appl. Phys. 69 (1991) 3605.
- [8] K. Asada, K. Sakamoto, T. Watanabe, T. Sameshima, S. Higashi, Jpn. Appl. Phys. 39 (2000) 3883.
- [9] Y. Tsunoda, T. Sameshima, S. Higashi, Jpn. J. Appl. Phys. 39 (2000) 1656.
- [10] S. Higashi, N. Ando, K. Kamisako, T. Sameshima, Jpn. J. Appl. Phys. 40 (2001) 731.
- [11] H. Watakabe, T. Sameshima, H. Kanno, T. Sadoh, M. Miyao, J. Appl. Phys. 95 (2004) 6457.
- [12] M.V. Fischetti, S.E. Laux, J. Appl. Phys. 80 (1996) 2234.
- [13] T. Sameshima, S. Usui, Mater. Res. Soc. Symp. Proc. 258 (1992) 117.